EMT Representation and Dynamic Performance of Composite Load Models in IBR-Based Power Systems

Hossein Ashourian
PGSTech
Montreal, Canada
hossein.ashourian@emtp.com

Alireza Masoom
Dep. of Networks Simulation
Hydro Quebec Research Institute
Varennes, Canada
masoom.alireza@hydroquebec.com

Jean Mahseredjian
Dep. of Electrical Engineering
Polytechnique Montreal
Montreal Canada
jean.mahseredjian@polymtl.com

Hanry Gras
PGSTech
Montreal, Canada
hanry.gras@emtp.com

***Abstract*— Accurate load modeling is essential for reliable power system analysis, especially in electromagnetic transient (EMT) simulations where fast, nonlinear dynamics must be faithfully represented. Traditional static models, such as the ZIP model, often overlook how actual loads respond during grid disturbances. This paper presents an EMT-compatible version of the WECC Composite Load Model (CMLD), expanding the phasor-domain model to include static, motor, and power-electronic load components within an EMT framework. This development enables the study of fault-induced delayed voltage recovery (FIDVR) and the interactions between dynamic loads and inverter-based resources (IBRs). Simulations on a modified IEEE 39-bus system show that substituting ZIP loads with the EMT-based composite model has a significant impact on post-fault voltage recovery and fault ride-through (FRT) performance in converter-based networks.**

***Index Terms*—EMT -detailed load, WECC, Composite Load Model, EMT.**

I. Introduction

Accurate load modeling plays a crucial role in ensuring reliable power system analysis, especially when it comes to EMT simulations [1][2]. These simulations require capturing fast, and nonlinear dynamics, which traditional load models often fail to represent effectively. For instance, the commonly used ZIP model treats load as a static function of voltage, neglecting the dynamic behaviors that occur during disturbances. This limitation makes it difficult to accurately simulate fault-induced phenomena, such as faults that induce delayed voltage recovery, and to differentiate between various end-use load types. To address these challenges, more comprehensive and physically realistic models like composite load models (CMLDs) have been developed [2]. These models incorporate a variety of load components, such as static ZIP elements, induction motors (both single-phase and three-phase), and power electronic devices, within a unified framework. One key motivation for developing CMLDs is their ability to replicate fault-induced delayed voltage recovery (FIDVR), a phenomenon in which voltage remains depressed for a prolonged period after fault clearance due to motor load stalls and subsequent reacceleration. Such events pose serious threats to voltage stability and are inadequately captured by static load models.

As power grids evolve, integrating higher levels of IBRs and large converter-dominated loads — such as data centers, electric vehicle charging stations, and cryptocurrency mining farms —becomes increasingly common. The dynamic and nonlinear nature of these emerging load profiles—often marked by unpredictable behavior—raises critical issues for system stability and protection coordination [3]. Despite the importance of advanced load models, developing, parameterizing, and validating CMLDs is a complex process. Challenges include understanding load interactions, accurately initializing dynamic states, and ensuring seamless integration with network analysis tools [5]. Among the various models available, the Western Electrical Coordinating Council (WECC) composite load model is one of the most widely used and trusted [6]. It provides a standard way to represent various types of loads and is included in several phasor-domain tools, such as PSLF, PSSE, and PowerWorld. For example, a CMLD model has been developed in [7] and [8] to study FIDVR phenomena in power systems using positive-sequence phasor-domain simulations. However, the application of this composite load model in EMT simulations remains uncommon and relatively unexplored. Most current work focuses on phasor-domain analysis, and electromagnetic transient (EMT)-based versions of the WECC CMLD are not yet widely available or validated. As a result, detailed studies on how loads interact with IBRs during faults and voltage recovery are limited. Expanding the use of CMLDs into EMT simulations is crucial for achieving more accurate analysis of FRT and post-fault voltage recovery in networks dominated by converters.

To bridge this gap, this paper introduces an EMT-compatible version of the WECC CMLD. The proposed EMT-based CMLD model combines three-phase and single-phase induction motors, power electronics, and static loads, instead of using traditional ZIP-based EMT load representations. This advancement enables detailed analysis of load behavior during various transient conditions. Using a modified IEEE 39-bus system, the paper examines how replacing traditional static ZIP loads with dynamic composite loads influences voltage recovery, load stability, and the performance of IBRs after faults.

In this paper, Section II recalls the models used for various load components with added information. Section III presents the initialization of the developed model. In Section VI, the proposed model is tested and validated with realistic results.

II. WECC Composite Load Modeling

The WECC Composite Load Model with Distributed Energy Resource (DER) representation (CMPLDWG) has become the benchmark structure for large-scale dynamic studies [2]. It combines an equivalent substation transformer, feeder impedance, shunt compensation, and multiple dynamic

979-8-3315-8138-1

and static load components to represent the electrical distance and diversity between transmission-level buses and end-use devices. The loads are primarily divided into two categories: electromechanical-based and power-controlled loads. For the first category, which includes motor types A-C, an EMT-detailed model is used to accurately represent the electromechanical dynamics of the machines. The second category, comprising electronic and static components along with a single-phase motor D, is modeled using physics-based

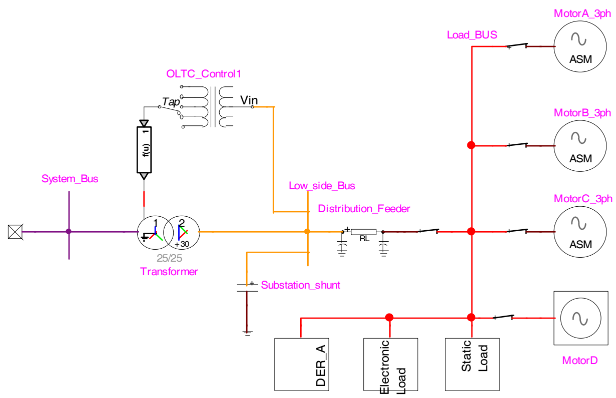

Fig. 1. Implementation of WECC composite load model with DER representation in EMTP.

techniques that produce active and reactive power references according to the component's behavior. The instantaneous-power theory is applied [9], where given the reference powers p^{ref} and q^{ref}, and the measured voltages v_d and v_q, the corresponding current references are calculated as follows

$$\begin{bmatrix} \mathrm{i}_d^{ref} \\ \mathrm{i}_q^{ref} \end{bmatrix} = \frac{1}{\mathrm{v}_d^2 + \mathrm{v}_q^2} \begin{bmatrix} \mathrm{v}_d & \mathrm{v}_q \\ -\mathrm{v}_q & \mathrm{v}_d \end{bmatrix} \begin{bmatrix} p^{ref} \\ q^{ref} \end{bmatrix} \tag{1}$$

The dq-axis currents are then transformed back to the three-phase reference frame via the inverse Park transformation. These three-phase reference currents are power-controlled current sources that supply the desired instantaneous power to the EMT network. This integrated method guarantees that power-controlled systems maintain correct steady-state power levels and respond smoothly and continuously to rapid voltage disturbances.

A conceptual schematic of the EMT-type model is shown in Fig. 1. The CMPLDWG model includes the following sub-modules:

- substation and feeder equivalent: RL feeder with optional shunt capacitors and on-load tap-changing (LTC) transformer providing low-side voltage regulation.
- Motor types A, B, and C: three classes of motors representing industrial drives, fan and pump loads, and large HVAC compressors.
- Motor type D: represents a single-phase induction motor, e.g., residential HVAC systems.
- static load: ZIP-type representation of resistive, lighting, and constant-power loads.
- electronic load: an aggregated representation of single-phase rectifier and power-electronic devices with undervoltage tripping logic.
- Distributed Energy Resource (DER_A): An optional inverter-based generation block, consistent with the WECC DER_A model, enabling representation of embedded PV or storage.

A. *Three-phase Motor Model*

Various types of three-phase induction motors are commonly used to represent end-use loads. In the CMPLDWG model, three distinct motor types, i.e., Motor A, Motor B, and Motor C, are employed to capture different dynamic load characteristics. Motor A models feature low-inertia, constant-torque loads, such as air conditioning compressors and positive displacement pumps. Motor B represents high-inertia, variable-torque loads typically found in commercial ventilation systems and air-handling units. Motor C is used for low-inertia, variable torque applications, such as standard centrifugal pumps. In the proposed model, users can select motors to represent using either single-cage or double-cage configurations. Each motor group also includes a two-stage protection scheme that emulates the aggregated response of contactors and under-voltage relays. Portions of the motor load disconnect when the voltage drops below the specified threshold values and reconnect once the voltage exceeds the corresponding reconnection values. All timers and thresholds are implemented as discrete-event logic synchronized with the EMT integration step (20-50 μs), ensuring smooth staged recovery. The phasor-domain parameters of Motor A to C are translated into their EMT equivalents, while maintaining electrical constants and dynamic behaviors, ensuring consistency between RMS and EMT models.

B. *Motor Type D*

Motor D in the CMPLDWG model represents the aggregated behavior of residential single-phase air-conditioning compressor motors. It is modeled algebraically, and it captures the thermal protection behavior of residential AC units. The model captures key nonlinear behaviors, such as stalling, tripping, and re-acceleration, consistent with laboratory observations of residential air conditioning units.

C. *Static Loads Model*

The static-load accounts for resistive and lighting devices and is modeled by the classical ZIP (constant impedance–current–power) formulation:

$$\mathrm{P}_{ZIP} = \mathrm{P}_n \left[p_1 \left(\frac{\mathrm{V}}{\mathrm{V}_n} \right)^2 + p_2 \left(\frac{\mathrm{V}}{\mathrm{V}_n} \right) + p_3 \right], \quad \sum_{i=1,2,3} p_i = 1 \tag{2}$$

$$\mathrm{Q}_{ZIP} = \mathrm{Q}_n \left[q_1 \left(\frac{\mathrm{V}}{\mathrm{V}_n} \right)^2 + q_2 \left(\frac{\mathrm{V}}{\mathrm{V}_n} \right) + q_3 \right], \quad \sum_{i=1,2,3} q_i = 1 \tag{3}$$

979-8-3315-8138-1

where P_{ZIP} and Q_{ZIP} are the active power and reactive power at the bus of interest, respectively; P_n and Q_n are nominal active and reactive powers at nominal voltage V_n. In EMT implementation, the active and reactive powers are injected using a current source.

D. Electronic Load Model

The electronic load components model the collective behavior of power electronic devices, such as variable-speed drives, rectifiers, and consumer electronics. According to the WECC specification, its voltage–power characteristic behaves as nearly constant power at the nominal voltage. Below a defined threshold, the power output decreases linearly to zero. A recovery factor governs partial reconnection once the voltage rises above the disconnection range. In EMT simulations, this component is implemented using a controlled current source that injects instantaneous active and reactive powers based on the voltage–power profile. Discrete-event logic is used to model undervoltage tripping and reconnection, synchronized with the EMT integration step.

E. DER Model

In the CMPLDWG, the DER represents aggregated inverter-based generation, typically rooftop photovoltaic (PV) systems or small battery units, connected at the low-voltage bus. In the EMT implementation, the DER is modeled following the structure of the WECC DER_A model [10], where the dynamic control system generates reference currents for the converter.

The DER_A control block computes the active and reactive current references, i_d^* and i_q^*, based on the reference active and reactive powers, P_{ref} and Q_{ref}, and the measured terminal voltages as shown in Fig. 2. These dq current references are then fed into the inner current-loop controller, which regulates the converter's output currents to track i_d^* and i_q^*. An averaged converter model is used, where the instantaneous switching behavior is neglected, and the inverter output is represented by its averaged dq-frame voltages. This approach accurately captures the dynamic response of the inverter control while maintaining a numerically efficient and stable simulation for large-scale EMT studies.

The model incorporates current limiting, reactive-priority logic, and low-voltage ride-through (LVRT) capability, which is consistent with the WECC DER_A specification. This implementation enables the DER to interact realistically with surrounding motor, static, and electronic loads, allowing for EMT-level analysis of active and reactive power recovery, current limitation, and grid-support performance during voltage disturbances.

III. Initialization of the CMPLDWG

Accurate and numerically stable initialization is crucial for large-scale EMT simulations that incorporate numerous nonlinear devices, such as machines, IBRs, and composite load models. In EMTP®, all system components—including synchronous machines, asynchronous machines, and converters—can be automatically initialized from the solved load-flow solution. During the pre-initialization stage, each power-controlled-based load branch is temporarily replaced with an equivalent R–L impedance that replicates its steady-state active and reactive power consumption at nominal voltage. In the time-domain initialization phase, the model's initial states of controllers and dynamic elements are set based on the calculated steady-state voltage magnitude and phase angle, ensuring a smooth and consistent transition from the load-flow solution to the EMT simulation.

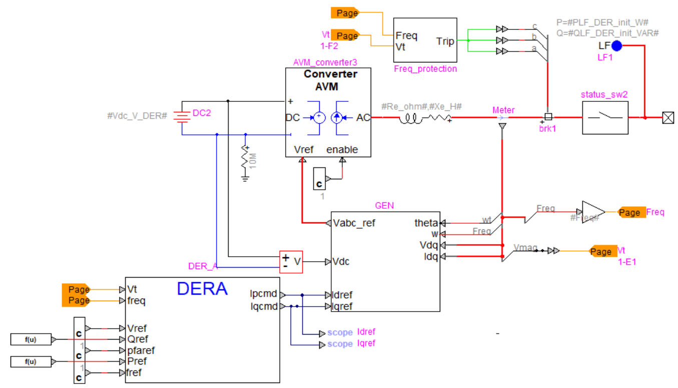

Fig. 2. Implementation of DER-A, schematic diagrams.

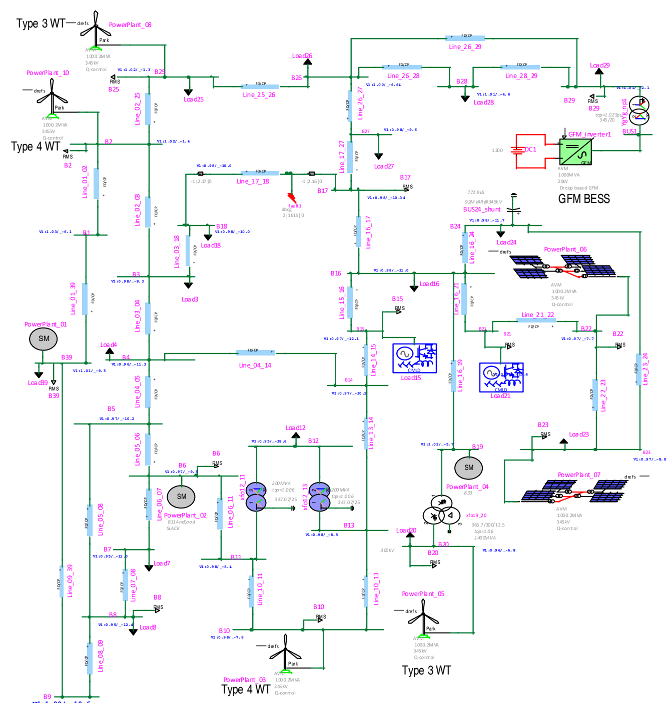

Fig. 3. IEEE-39 bus system with two types of loads (1) conventional PQ loads, (2) WECC CMLD load on buses B15 and B21.

IV. Simulations And Results

The developed EMT-based composite load model was tested using a modified version of the IEEE-39 bus system based on the initial version of [11], which was adapted to simulate conditions dominated by IBRs, as shown in Fig. 3. This system includes three traditional synchronous generators (SGs), four wind power plants (Types III and IV), and two PV parks, all operating in grid-following mode. Additionally, a battery energy storage system (BESS) configured in grid-forming mode provides power to bus B29. SGs, PV, wind, and BESS models, as well as their controllers, are implemented using generic models provided in the EMTP® library[12][13]. To mimic real-world load behavior, two WECC CMLDs, referred to as Load15 and Load21, were implemented at buses B15 and B21, respectively. The details of these loads are summarized in Table 1, and their steady-state active and reactive powers were calibrated to match the original system data. This comparison examines how the new CMLD behaves compared to the traditional ZIP model during a specific electrical disturbance. The test involved simulating a three-phase fault on Line_17_18 at $t = 2s$, then disconnecting the line from both ends at $t = 2.1s$.

Fig. 4 and Fig. 5 illustrate the active and reactive power responses at Load15, primarily electronic, and Load21, mainly motoring, respectively. Before the fault occurred, both models showed similar steady power levels at their respective locations. However, once the fault happened, their behaviors diverged. For Load15, the ZIP model quickly returned to its normal power level after the disturbance. On the other hand, the composite load model shows a more complex recovery process. The electronic components respond quickly, but some loads disconnect due to undervoltage protection and delays in converter restart. This caused the active power to remain below normal for a few cycles, while the reactive power gradually recovered as the converters re-energized. Overall, the composite load's power recovery was smoother but took longer than the ZIP model.

For Load21, the ZIP model's active and reactive powers return to their normal levels after the fault is cleared. In contrast, the CMLD, which mainly consists of induction motors, shows noticeable electromechanical transients. When the fault occurs, the motors stall, resulting in a sharp drop in active power and a spike in reactive power demand. As the voltage recovers, the motors reaccelerate, leading to transient inrush currents and oscillations in both active and reactive power. These oscillations are mostly pronounced between about 2.1 s and 2.4 s and gradually dampen as the motors settle into steady operation.

As illustrated in Fig. 6, during the fault, the reactive power output of the PV park increases even though it operates in Q-control mode with zero reactive power reference. This occurs due to the FRT logic, which injects a reactive current to support voltage recovery. After the fault is cleared and the stalled motors at Load21 start reaccelerating, their high inrush currents cause a secondary voltage dip. This dip pushes the PV inverter into its LVRT region. During this transient, the inverter temporarily limits active power output while continuing to inject reactive current. The combined effect of motor reacceleration and PV LVRT operation slows down the overall voltage recovery and the restoration of active power. This underscores the importance of capturing these coupled load and inverter dynamics in EMT simulations.

For the ZIP load case, the PV park only switches to FRT mode once, i.e., during the initial fault, and then immediately resumes normal operation afterward.

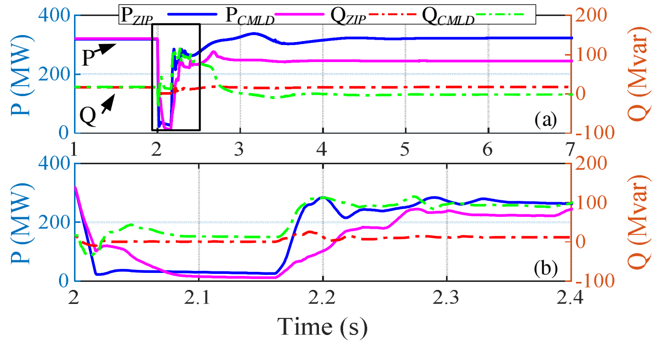

Fig. 4. Comparison of active and reactive powers between the ZIP and CMLD load models at Load15, mainly the electronic load. (b) provides a zoomed-in view of (a) around 2.2s.

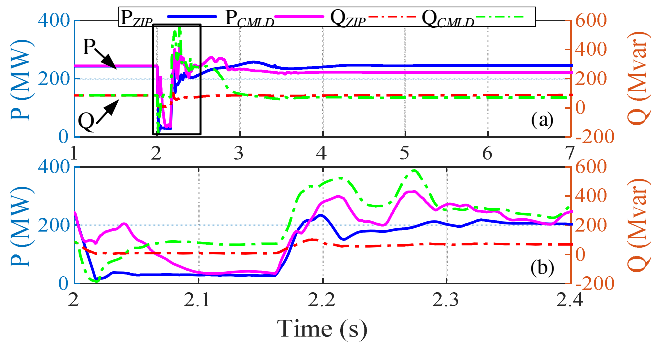

Fig. 5. Comparison of active and reactive powers between ZIP and CMLD load models at Load21, mainly motoring loads. (b) provides a zoomed-in view of (a) around 2.2s.

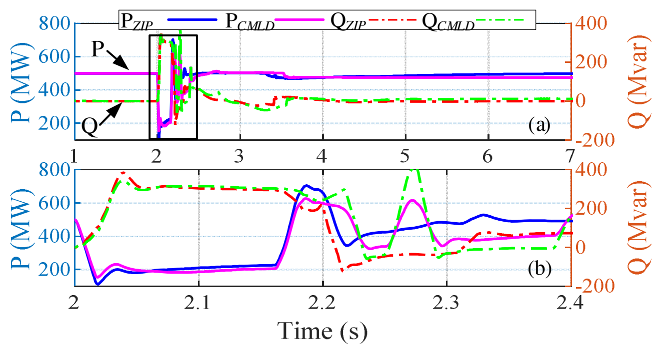

Fig. 6. Comparison between active and reactive powers generated in PowerPlant_06 (PV Park) for ZIP and CMLD load models.

This suggests an idealized recovery that doesn't consider the secondary voltage dips often observed in more complex load scenarios.

As depicted in Fig. 7 and Fig. 8, the voltage at bus B15 and bus B21 dips below the motor stall threshold during the fault, leading to partial disconnection of motor loads. Once the voltage recovers, some motors reaccelerate simultaneously, creating inrush currents that cause further secondary voltage dips. This effect is particularly noticeable at Load21, where motor loads account for over 80% of the total demand. The combined impact of stalling, tripping, and reaccelerating motors causes oscillations during voltage recovery, underscoring how buses dominated by motors are particularly

979-8-3315-8138-1

susceptible to severe voltage disturbances. In contrast, for the ZIP load, the voltage quickly bounces back to pre-fault levels without such secondary dips.

TABLE 1 : THE LOAD PROFILE FOR LOAD15 AND LOAD21

Load type	Load15	Load21
Motor A	10 %	50 %
Motor B	10 %	20 %
Motor C	0	20 %
Static load	5 %	0
Electronic load	75 %	10 %
Total	500MVA, 320 MW	800MVA, 247 MW

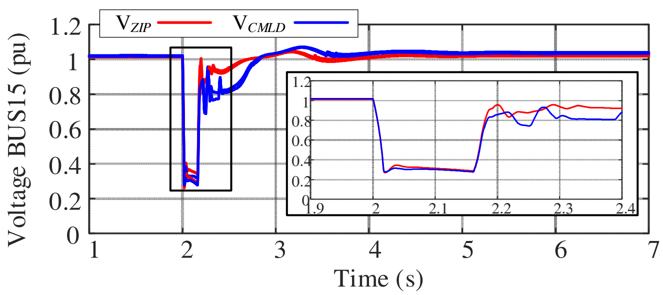

Fig. 7. Comparison of RMS voltage profile between ZIP and CMLD load models in Load15.

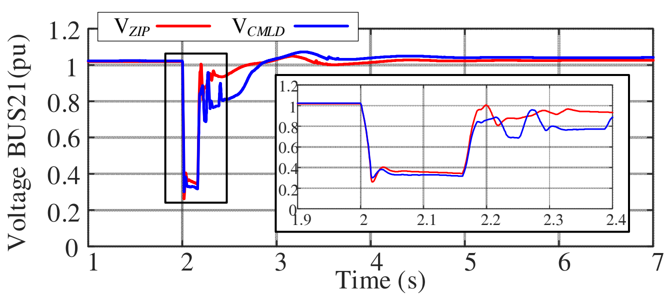

Fig. 8. Comparison of RMS voltage profile between ZIP and CMLD load models in Load21.

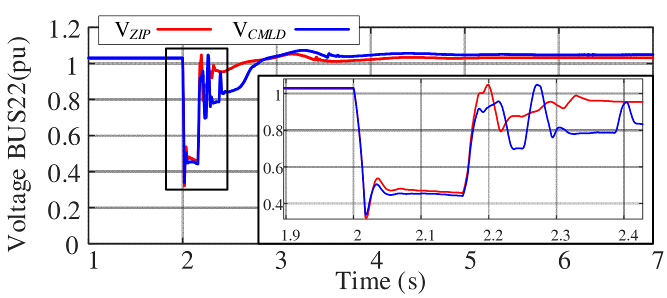

Fig. 9. Comparison of RMS voltage profile between ZIP and CMLD load models on bus B22 (PowerPlant_06).

CONCLUSION

This study examined the behavior of ZIP and CMLD load models during fault conditions, focusing on their dynamic responses. Both models had similar operating points before the fault, but differences emerged after the disturbance. The CMLD model reflected important phenomena such as load disconnection, motor stalling, inrush currents, and delayed voltage recovery, which the ZIP model did not capture. These effects were especially evident in heavily motorized areas like Load 21. Additionally, the interaction between dynamic loads and inverter-based resources was more pronounced with the CMLD model, causing IBRs to switch in and out of fault-ride-through mode and resulting in system responses that diverged from ZIP-based results. Overall, this emphasizes the need for accurate composite load models to realistically simulate post-fault dynamics and improve the reliability of stability assessments in systems with many converters.

Future work will aim to improve the study by using the proposed model for more complex load profiles. In addition, the study will be more meaningful when validated on large-scale power systems.

REFERENCES

[1] D. N. Kosterev, C. W. Taylor and W. A. Mittelstadt, "Model validation for the August 10, 1996, WSCC system outage," IEEE Transactions on Power Systems, vol. 14, no. 3, p. 967–979, 1999.

[2] North American Electric Reliability Corporation (NERC), *Reliability Guideline: Developing Load Model Composition Data*, Atlanta, GA, USA, June 2019. [Online]. Available: https://www.nerc.com/comm/RSTC_Reliability_Guidelines/Reliability_Guideline_-_Load_Model_Composition_-_2017-02-28.pdf

[3] North American Electric Reliability Corporation (NERC), *Reliability Guideline: Characteristics and Risks of Emerging Large Loads*, Atlanta, GA, USA, June 2023. [Online]. Available: https://www.nerc.com/comm/RSTC_Reliability_Guidelines/Whitepaper%20Characteristics%20and%20Risks%20of%20Emerging%20Large%20Loads.pdf

[4] Electric Power Research Institute (EPRI), *Technical Reference on the Composite Load Model*, Palo Alto, CA, USA: EPRI, 3002018056, March 2019. [Online]. Available: https://www.epri.com/research/products/000000003002019209

[5] F. Bu, Z. Ma, Y. Yuan and Z. Wang, "WECC Composite Load Model Parameter Identification Using Evolutionary Deep Reinforcement Learning," in *IEEE Transactions on Smart Grid*, vol. 11, no. 6, pp. 5407-5417, Nov. 2020, doi: 10.1109/TSG.2020.3008730.

[6] Z. Ma, Z. Wang, Y. Wang, R. Diao and D. Shi, "Mathematical Representation of WECC Composite Load Model," in *Journal of Modern Power Systems and Clean Energy*, vol. 8, no. 5, pp. 1015-1023, September 2020, doi: 135833/MPCE.2019.000296.

[7] N. Castrillón, C. González, P. Pourbeik and E. Gallego, "Developing a Composite Dynamic Load Model for the Colombian Power System," 2025 International Conference on Artificial Intelligence, Computer, Data Sciences and Applications (ACDSA), Antalya, Turkiye, 2025, pp. 1-6.

[8] A. Cisco Sullberg, M. Wu, V. Vittal, B. Gong and P. Augustin, "Examination of Composite Load and Variable Frequency Drive Air Conditioning Modeling on FIDVR," in IEEE Open Access Journal of Power and Energy, vol. 8, pp. 147-156, 2021, doi: 10.1109/OAJPE.2021.3071692.

[9] Modelling and Aggregation of Loads in Flexible Power Networks Technical report, CIGRE Working Group C4.605, February 2014

[10] "The new aggregated distributed energy resources (DER_A) model for transmission planning studies: 2019 update," Elect. Power Res. Inst., Palo Alto, CA, USA, Rep. 3002013498, 2019.

[11] A. Haddadi, J. Mahseredjian, "Power System Test Cases for EMT-type Simulation Studies," CIGRE WG C4.503 brochure, August 2018.

[12] H. Ashourian and H. Gras, "WECC PV Park Model," EMTP, 2022. [Online]. Available: https://www.emtp.com/documents/EMTP%20Documentation/doc/Renewables/WECC_PV_Park_Models.pdf

[13] H. Ashourian and H. Gras, "Three-phase Grid Forming Inverter,", EMTP, 2023. [Online] Available: https://www.emtp.com/documents/EMTP-Documentation/doc/toolboxes/powerelectronics/gfm-inverter.pdf